DOI: https://doi.org/10.15407/rpra29.01.015
UDC 537.86+621.37

**A. Kirilenko[1,2], S. Steshenko[1,2], Y. Ostryzhnyi[1], V. Derkach[1]**

[1] O.Ya. Usikov Institute for Radiophysics and Electronics NAS of Ukraine
12, Acad. Proskury St., Kharkiv, 61085, Ukraine
[2] V.N. Karazin Kharkiv National University
4, Svobody Sq., Kharkiv, 61022, Ukraine
E-mail: aakirilenko@ukr.net; sergiy.steshenko@gmail.com;
eruost@ukr.net; derkach@ire.kharkov.ua

# EIGEN-OSCILLATIONS OF PLANAR-CHIRAL BILAYER OBJECTS GIVE RISE TO ARTIFICIAL OPTICAL ACTIVITY

***Subject and Purpose.*** *The research focuses on how the resonance frequencies, the Q-factor of resonances, and the polarization plane rotation ability are influenced by the topology of individual components of a planar-chiral double-layer object consisting of a pair of conjugated irises having rectangular slots and accommodated in a circular waveguide.*

***Methods and Methodology.*** *All the numerical results are obtained by the mode-matching technique (MMT) and the transverse resonance method on the basis of our own proprietary MWD-03 software package.*

***Results.*** *By the waveguide example, it has been shown that the internal structure of individual components and dihedral symmetry of the conjugated bilayer allow all the conclusions of the spectral theory (theory of eigen-oscillations) to be carried over to all the objects of the type. On the other hand, these objects behave as symmetric two-port waveguide components with conventionally "symmetric" and "antisymmetric" eigen-oscillations. The mutual coupling of these eigen-oscillations depends on the bilayer parameters. Where the frequencies of these eigen-oscillations are close enough, the polarization plane rotation and the transmission bandwidth reach their highest. It has been demonstrated that as a slot number increases, the resonance frequency decreases. The theoretical results have been confirmed by the measurements at the X range of frequencies for pairs of conjugated irises with various numbers of rectangular slots.*

***Conclusions.*** *A pair of conjugated chiral irises can rotate the polarization plane. The iris topology, iris spacing, and the mutual rotation angle alter resonance frequencies. The resonance frequencies can be reduced by increasing the rectangular slot length and/or slot number. Even though they have not longitudinal symmetry, such objects have properties of two-port waveguide components. In particular, the phase shift of their reflection and transmission coefficients is modulo 90°. Besides, a possibility exists to divide eigen-oscillations into conventionally "symmetric" and "antisymmetric" based on the proximity of their fields to those whose type of symmetry is known beforehand. This makes it possible to approximate the reflection and transmission coefficients through corresponding eigenfrequencies.*

***Keywords:*** *eigen-oscillations, bilayer objects, 3D-chirality, artificial optical activity, dihedral symmetry, planar-chiral irises, polarization converters.*

Citation: Kirilenko, A., Steshenko, S., Ostryzhnyi, Y., Derkach, V., 2024. Eigen-oscillations of planar-chiral bilayer objects give rise to artificial optical activity. *Radio Phys. Radio Astron.*, **29**(1), pp. 15—25. https://doi.org/10.15407/rpra29.01.015

Цитування: Кириленко А., Стешенко С., Острижний Є., Деркач В. Власні коливання в планарно-кіральних двошарових об'єктах породжують штучну оптичну активність. *Радіофізика і радіоастрономія*. 2024. Т. 29, № 1. С. 15—25. https://doi.org/10.15407/rpra29.01.015

## Introduction

Among the metamaterials that provide artificial optical activity (AOA), bilayer structures occupy a special place with the vast majority of publications. Dating back to work [1], a variety of planar chiral metasurfaces have been proposed. Square cells (meta-atoms) of the periodic structures are tailored using thin metal patches or slotted screens (fish-net structures). Metasurface cells should not possess symmetry planes, i.e. they are supposed to be planar-chiral forms with $C_4$ rotational symmetry. See, for example, angular-shift rosettes in Fig. 1, *a* [1] with 3D chirality occurring at nonzero angular shift. Such bilayers bestow the most fascinating properties when the first and second layers have conjugated geometries (Fig. 1, *b*) [2]. Also, worthy of mention are composite bilayer metasurfaces (Fig. 1, c) [3] containing double-mirror-symmetry metal inserts improving matching and objects with S-shaped metal patches providing the double-band AOA phenomenon (Fig. 1, *d*) [4]. The affinity of the properties gives rise to waveguide applications of bilayers as three-dimensional chiral devices (Figs. 1, *e* [6] and 1, *f* [7]). The conclusions made further in the paper and concerning eigen-oscillations of such open microwave structures with a discrete spatial spectrum are valid for each object in Fig. 1. All the bilayers in Fig. 1 except the one in Fig. 1, *a* have $D_4$ (dihedral) symmetry. Many other examples can be found, e.g., in [5].

For the plane-wave normal incidence, the aforementioned bilayers provide the polarization plane (PP) rotation in the transmitted field and the absence of cross-polarized waves in the reflected field. Also, this is the case for 2D-periodic structures arranged in hexagonal lattices when the scatterer geometry has both rotational ($C_6$) and required translation symmetry. An AOA example in the hexagonal lattice case is given in [8].

Normally, the AOA analysis reduces to studying distributions of surface electric (for patches) or magnetic (for slots) currents in the two layers of the meta-atom cell. Then, by analogy with the Faraday effect, the equivalent parameters of the "imaginary homogeneous" medium are reconstructed. Work [6] uses a waveguide example and interprets the AOA phenomenon in terms of special eigen-oscillations inside the internal gap of a bilayer object. We call them dihedral eigen-oscillations because of dihedral symmetry of their eigenfields. In principle, this concept is consistent with early works [9] on bilayer screens.

Below, the above-mentioned concept is generalized to waveguide bilayers with arbitrary-order dihedral symmetry. We will demonstrate how the resonance properties of meta-atom components themselves affect the AOA manifestation. The waveguide example is very important in the practical sense because it, for instance, broadens the application scope of compact polarization rotators based on slotted irises [10] or corrugated flanges [7]. Its scientific importance is in opening up research prospects for further exploration of the $D_n$ symmetry cases with arbitrary $n$ rather than $n = 2, 4, 6$ for two-layer periodic lattices only.

In this paper, we consider a bilayer planar-chiral pair from Fig. 2. Each iris has $n$ rectangular slots uniformly distributed in azimuth. We use $a$ and $b$ notations for, respectively, the $x$ and $y$ dimensions of the rectangular slot sides, as shown in the lower left corner of the first iris in Fig. 2.

All the presented numerical results are due to our own proprietary MWD-03 software package enabling us to employ the mode matching technique (MMT) and the transverse resonance method for the electromagnetic analysis of 3D boundary-value problems with piecewise coordinate boundaries, including the eigen-oscillation analysis in the complex frequency plane. To calculate the plane junctions (PJs) between the waveguides in Cartesian and polar coordinates, the approach proposed in [11] is adopted. The calculation accuracy is controlled with parameter $f_{\max}$ which bounds from above the values of cutoff frequencies of the projection bases of all regular waveguides in the structure. In most theoretical calculations throughout the work, $f_{\max} = 100$ GHz, which is sufficient for high-quality results. But sometimes to get a detailed comparison with the experiment, $f_{\max} = 340$ GHz was also used. The $f_{\max}$ increase from 100 to 340 GHz raises the resonance frequency by no more than 400 MHz.

The present work is a continuation and an essential extension of conference paper [12]. We seek to control the artificial optical activity characteristics by altering the topology of a bilayer of conjugated planar-chiral irises. A primary focus is on the general spectral properties of bilayers of waveguide irises and planar screens.

## 1. General features of eigen-oscillations of a bilayer

Let us consider two closely spaced objects accommodated inside a certain waveguide line or in the free space with a discrete mode basis which we think of as either waveguide modes or Floquet waves. As known, the dispersion equation that determines the set of eigen-oscillations of such an "open" object is

$$\det(\mathbf{I} - \mathbf{RE}\hat{\mathbf{R}}\mathbf{E}) = 0, \quad (1)$$

where $\mathbf{R}$ and $\hat{\mathbf{R}}$ are the generalized matrices describing the multiple reflection of waveguide modes or Floquet waves from the external components (interfaces) of the "bilayer" and $\mathbf{I}$ is the identity matrix. The diagonal matrix $\mathbf{E} = \mathbf{E}(l)$ describes the process of propagation or reactive attenuation of these waves in the bilayer gap of size $l$.

In some cases, Eq. (1) can split in two factors. Specifically, in the case of an ordinary longitudinally symmetric object, $\mathbf{R} = \hat{\mathbf{R}}$, and Eq. (1) splits into the pair

$$\det(\mathbf{I} \pm \mathbf{RE}) = 0 \quad (2)$$

describing the well-known oscillations with PMW ("perfect magnetic wall" in the plane of symmetry $z = 0$) or with PEW ("perfect electric wall", $z = 0$). They are solutions to Eq. (2) with sign "–" or sign "+", respectively. Eigen-oscillations with PEW and PMW in the plane of symmetry have different eigenfrequencies.

A particular case of the longitudinally symmetric object of the kind is a *single iris or a screen as a bilayer of interfaces.* They also are bilayer forms and have corresponding pairs of eigen-oscillations [13]. The eigen-oscillations with PMW are the origin of the well-known "half-lambda" resonances of slots in irises or in screens. The oscillations with PEW usually have a very high $Q$ and could not be detected experimentally for a long time because of their location right before the multimode band. These eigen-oscillations of bilayers provide the phenomenon of extraordinary optical transmission (EOT) through below-cutoff holes in waveguide irises or in perforated screens [14].

Consider now a *bilayer of irises or screens*. Suppose that both bilayer components are identical and show planar chirality. In this case, they can form two kinds of 3D chiral objects that show the AOA. The counterparts can be either "conjugated" (with dihedral symmetry) or azimuthally shifted with respect to each other about the longitudinal axis. Some essential differences in the electromagnetic behavior of these pairs are numerically examined in [15].

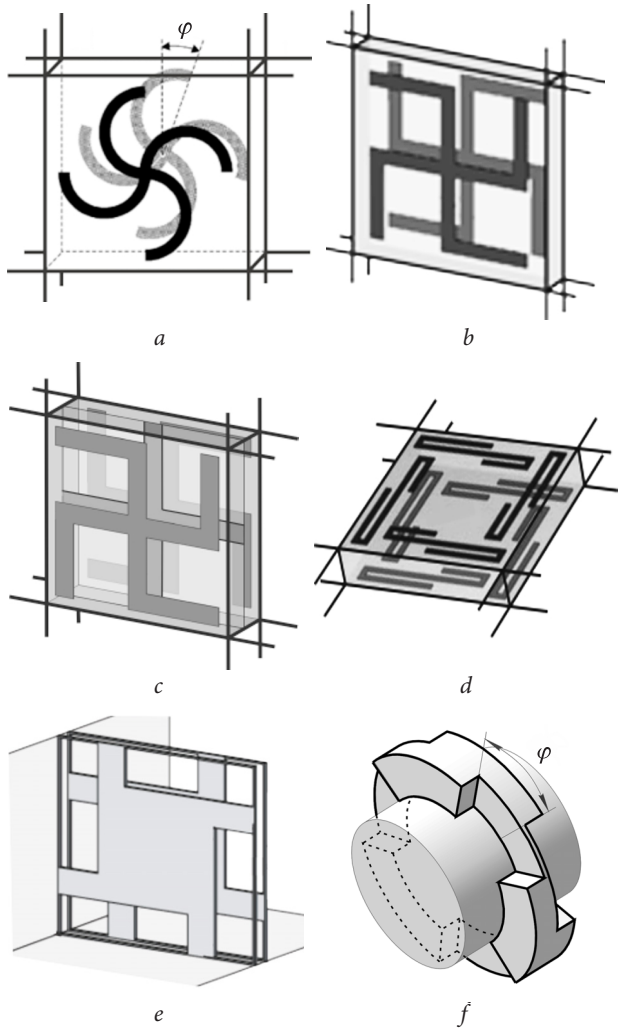


***Fig. 1.*** Investigated examples of bilayer structures

The fundamental difference between these two objects from a microwave standpoint is that only the conjugated variant obeys the properties of a symmetric two-port network, as will be shown below.

Let in a bilayer structure, the second iris (layer) be given by the rotation of its counterpart through $\pi$ about the $y$-axis and through an angle $\varphi$ about the structure axis $z$. These transformations correspond to the definition of a dihedral symmetry object. If the first iris has rotational symmetry $C_n$, then the bilayer of the two conjugated irises has dihedral symmetry $D_n$.

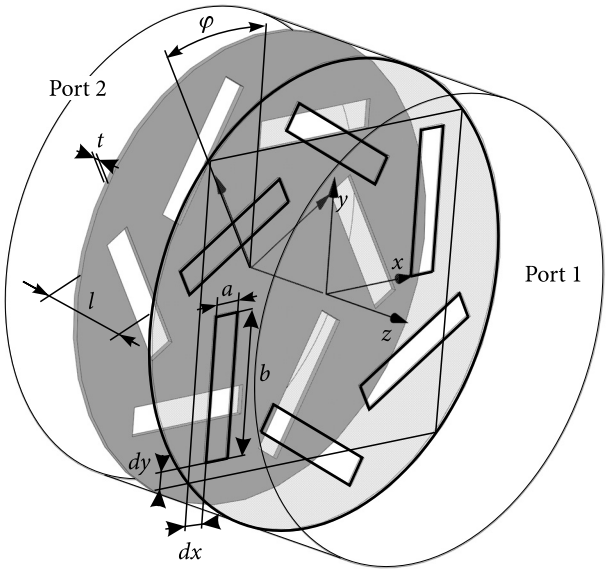


***Fig. 2.*** A pair of conjugated multislot planar-chiral irises with dihedral symmetry

According to the scattering problem solution in the lossless case, at the output port of the illuminated object with rotational symmetry $C_n$, $n \geq 3$, the linearity of the incident wave is preserved [9]. The real angle $\alpha$ of the PP rotation comes from

$$\tan\alpha = \operatorname{Re} S_{21}^{(\text{cross,co})} \Big/ \operatorname{Re} S_{21}^{(\text{co,co})} \qquad (3)$$

and must be found numerically. It is determined by the frequency, the constitutive parameters of the object, and its geometry. Here $S_{21}^{(\text{cross,co})}$ and $S_{21}^{(\text{co,co})}$ are the transmission coefficients into the cross- and co-polarized modes (waves), respectively.

If the scatterer possesses dihedral symmetry, the relation

$$\arg S_{11}^{(\text{co,co})} = \arg S_{21}^{(\text{cross,co})} \pm \pi/2 \qquad (4)$$

is satisfied. This is the reason to consider such an object as a two-port network of special symmetry.

On the contrary, a pair of identical non-conjugated planar-chiral irises with a mutual angular shift, which also provides the AOA, is an asymmetric two-port network. For it, relation (4) is not satisfied.

Next, to further investigate the AOA phenomena, we only consider objects with $D_n$ symmetry, $n \geq 4$. In this case, (a) the scattered field polarization in the far zone remains linear, (b) the effect of the PP rotation does not depend on the polarization of the incident mode, (c) there are no cross-polarized modes in the reflected field [16], and (d) the structure has the widest single-mode frequency band which is limited from above by the cutoff frequency of the $TM_{11}$ mode.

Note that the evanescent modes inside the bilayer gap play a decisive role in the excitation of eigen-oscillations and determine their distinctive features. Thus, for conventional resonators at regular waveguide sections, the real parts of neighboring eigenfrequencies generated inside the bilayer gap move downward together as the gap increases. However, the first pair of the oscillations formed in the bilayer narrow gap behave out-of-standard due to the intense interaction of the evanescent fields. In the considered dihedral case, the spectral lines can converge or diverge depending on the width of the gap between the meta-atom components in different layers. This property bestows a double-hump shape on the AOA curves.

## 2. Resonances of bilayer components

First of all, we turn to resonances of a single iris in the structure in Fig. 2 which one way or another affect the bilayer excitation governed by the solutions of Eq. (1). In this case, **R** is the reflection matrix of multichannel line modes incident on the plane junction (PJ) with the circular waveguide, where the multichannel line consists of $n$ small-size rectangular waveguides. According to [13], such PJs have aperture eigen-oscillations with complex-valued frequencies $f_{\text{eigen,PJ}}$ close to the cutoff frequency of the high-order $TM_{11}$ mode of the circular waveguide. For example, if the circular waveguide radius is $R = 16$ mm, the slot sides are $a = 12$ mm and $b = 1$ mm, and $n = 6$, this PJ is characterized by a pair of degenerate cross-polarized aperture oscillations at the frequency $f_{\text{eigen,PJ}} = (11.41 - i0.0008)$ GHz. This eigenfrequency value was obtained by the MMT method. It is a pole of characteristic Eq. (1) for the irises formed by the mentioned plane junctions.

Let the iris thickness be $t = 2.5$ mm. Two aperture oscillations inherent to the input and output PJs come into the interaction. Altogether, a set of six slots participating in the event yields a symmetric oscillation at $f_{\text{eigen,iris}}^{+} = (11.22 - i0.04)$ GHz and an extremely high-$Q$ antisymmetric oscillation at $f_{\text{eigen,iris}}^{-} = (11.4262 - i3.12\cdot10^{-6})$ GHz located immediately before the cutoff frequency $f_{\text{cut}}(TM_{11}) = 11.4265$ GHz of the first high-order mode of the circular waveguide.

The resonance frequencies of a single multi-slot iris and the bandwidths are listed in order of increasing $n$ in Table 1 [12]. It turns out that the resonance frequencies are quite close to $\mathrm{Re}\left(f^{+}_{\mathrm{eigen,iris}}\right)$ despite the fact that the $\mathrm{Im}\left(f^{+}_{\mathrm{eigen,iris}}\right)$ values are rather large. It was shown that 1) the slot number growth reduced the resonance frequency and the $Q$-factor, 2) the slot narrowing had little effect on the characteristics, and 3) resonances of thin irises, compared to thick ones, were shifted down in frequency and $Q$.

## 3. Eigen-oscillations and resonances of a dihedral pair

The interaction of two planar-chiral irises adds new pairs of eigen-oscillations with corresponding resonances on the frequency response. *The fundamental difference of such a 3D chiral unit lies in the rotation of the polarization plane of the transmitted field relative to the incident field.* For this reason, the corresponding eigen-oscillations with different PPs of the radiated at the outer ports eigenfields were called *dihedral* oscillations. As a microwave component, such a bilayer is still a two-port network, and its frequency response can be approximately described by the analytical representations based on a pair (or more) of eigenfrequencies [17] (see Section 5).

The device under consideration is characterized by resonances formed due to the peculiarities of both topological components. They are resonances of the irises (screens) themselves and resonances formed in the gaps between them. Both are well recognized in the 2D patterns (Fig. 3) of the reflection coefficient $S_{11}(f, l)$ for $R = 16$ mm, $n = 6$, $t = 0.1$ mm, $a = 12$ mm, $b = 0.5$ mm, and $dy = 0$. The bands of good matching are shown dark grey. The bands of strong reflection are shown white. Fig. 3 illustrates the cases of non-chiral (Fig. 3, *a*) and chiral (Fig. 3, *b*) irises. When $dx = (R\sqrt{2} - a)/2 \approx 5.31$ mm (Fig. 3, *a*), there exist $2n$ mirror-symmetry planes for the irises and $2n + 1$ such planes for the collective 3D object. Fig. 3, *b* displays the case of maximum ($dx = 0$) shifts of the slot centers from the centers of the sides of a square inscribed in the cross-section of the circular waveguide.

Near $\mathrm{Re}\left(f^{+}_{\mathrm{eigen,iris}}\right)$ at 9.6 GHz for $dx \approx 5.31$ mm and 10.6 GHz for $dx \approx 0$, apparent bands of good matching are observed in both Figs. 3, *a* and *b* for large gaps, where the near fields of the irises are practically evanescent. The "iris resonance" line is crossed by several "gap resonance" lines arrayed along $l$ at approximately a $\lambda_g/2$ interval, which is the half-wavelength of the dominant $\mathrm{TE}_{11}$ mode.

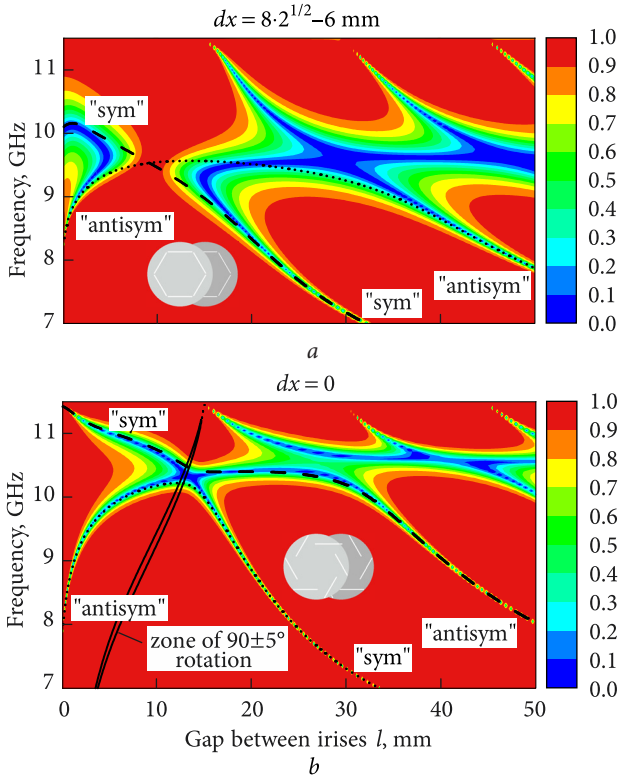


***Fig. 3.*** Reflection coefficient $S_{11}(f, l)$ of a bilayer consisting of 6-slot non-chiral (*a*) or chiral (*b*) irises in the gap-frequency coordinates

Fig. 3, *a* corresponds to a longitudinally symmetric structure with non-chiral irises, the dashed and dotted curves represent the real parts of the first two eigen-oscillations of the bilayer. In this case, the eigen-oscillations with PEW and PMW in the plane of symmetry are independent, for they are solutions of different boundary value problems. Therefore, the $\mathrm{Re}(f_{\mathrm{eigen}})$ curves for symmetric and antisymmetric eigen-oscillations can meet. The meeting is viewed at the gap $l = 9.2$ mm. Around this value of the gap, within the interval $l = 8.4$ to 10.6 mm, a strong reflection is revealed over the entire single-mode frequency band.

The structure analyzed in Fig. 3, *b* does not have longitudinal symmetry. The $\mathrm{Re}(f_{\mathrm{eigen}})$ curves in Fig. 3, *b* represent conventionally antisymmetric and symmetric eigen-oscillations of the bilayer in this case. We define eigen-oscillations as conventionally symmetric or antisymmetric depending on the proxi-

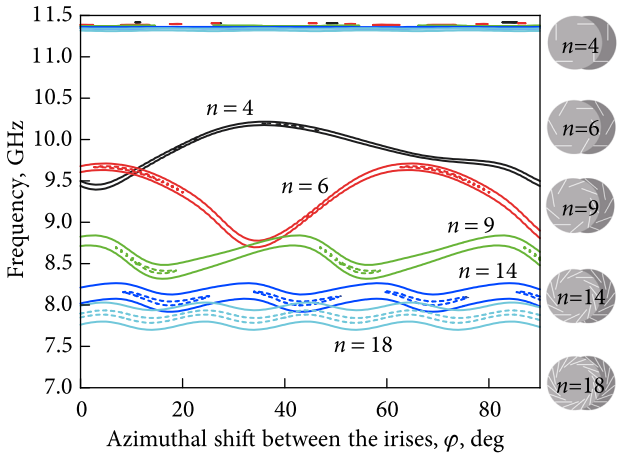


***Fig. 4.*** The action of azimuthal shift between planar-chiral irises at the level of transmitted cross-polarized mode for different slot numbers (marked on the graphs)

mity of their fields to those whose type of symmetry is known beforehand. That is, we call an eigen-oscillation conventionally symmetric (or "symmetric" in quotes) if the angle between its electric field vectors at the output ports and at largest amplitude peaks is acute. If obtuse, an eigen-oscillation is called conventionally antisymmetric ("antisymmetric" in quotes). For each eigen-oscillation of the first pair, there is a gap value at which this angle equals 90°. These are points where, by our definition, the eigen-oscillations change the type of conventional symmetry. At frequencies close to the corresponding $\mathrm{Re}(f_{\mathrm{eigen}})$, the PP rotates by 90° in the corresponding scattering problem. The zone of the PP rotation through $90 \pm 5°$ is also seen (Fig. 3, *b*).

The most fascinating region in Fig. 3, *b* is the area of small gaps, where the irises interact by their near fields, and the AOA phenomenon occurs. There the simple dependences for large *l* are violated.

The chirality introduction dramatically changes the frequency response behavior. The reflection bands are replaced by the bands of good matching as the dashed and dotted lines of $\mathrm{Re}(f_{\mathrm{eigen}})$ approach each other (compare Figs. 3, *a* and *b*). A similar phenomenon was investigated analytically and called the "inter-coupling" of converging eigen-oscillations [18]. The suggested [19] analytical interpretation of the "mode spectrum transformation" for open objects brought remarkable practical achievements.

In addition, the geometric chirality enhancement from its absence (Fig. 3, *a*) to a maximum (Fig. 3, *b*) raises the *Q*-factor of the resonances of both types.

## 4. Bilayer topology as a factor of AOA control

The interaction between the separate irises within the bilayer gap depends radically on the spectrum of waveguide modes actually excited between the irises. Specifically, when the dominant $\mathrm{TE}_{11}$ mode of the circular waveguide is incident, the interaction is carried out by the $\mathrm{TE(TM})_{|pn\pm1|,q}$ modes, $p = 0, 1, 2, \ldots$ and $q = 1, 2, \ldots$ due to $C_n$ symmetry of the components. It is clear that for $n = 3$, the single-mode frequency band is terminated by the $\mathrm{TE}_{21}$ mode cutoff frequency. But for $n \geq 4$, the single-mode operation holds up to $f_{\mathrm{cut}}(\mathrm{TM}_{11})$. Most importantly, as the slot number grows, the waveguide mode spectrum inside the gap becomes increasingly sparse until finally only three parts of the mode spectrum remain under interaction. These are 1) a cross-polarized pair of the dominant $\mathrm{TE}_{11}$modes, 2) a pair of the first, slightly decaying high-order $\mathrm{TM}_{11}$ modes, and 3) a lot of fast decaying $\mathrm{TE}_{1q}$ and $\mathrm{TM}_{1q}$ modes, $q = 2, 3, \ldots$ So, with large *n*, the decisive role in forming the collective frequency and polarization responses of 3D chiral bilayers in a circular waveguide is played by the quadruple of the $\mathrm{TE}_{11}$ and the $\mathrm{TM}_{11}$ modes of horizontal and vertical polarizations.

In our analysis of the effect caused by the azimuthal shift of bilayer components, we only focus on maximum-chirality irises. Due to the rotational symmetry, the azimuthal shift $\varphi$ dependences (see Fig. 2) have a $2\pi/n$ period.

Fig. 4 contains information on the $\mathrm{TE}_{11}$ cross-component level in the transmitted field at the first resonance of the multislot planar-chiral bilayer in the single-mode frequency band as *n* increases. The geometry parameters are $R = 16$ mm, $l = 1$ mm, $t = 0.1$ mm, $dx = dy = 0$, $a = 10$ mm, and $b = 0.5$ mm. The different-*n* lines display the contours of the $TE_{11}^{inc} \Rightarrow TE_{11}^{cross}$ conversion values at 0.5 (solid lines) and 0.8 (dashed lines) levels of the transmitted cross-polarized wave. So, the dashed lines circumscribe a strong conversion into the cross-polarized mode.

For the first resonance, the most pronounced resonance frequency oscillations with a change in $\varphi$ are observed for $n = 4$. Such resonance frequency oscillations are practically unnoticeable for $n = 18$, when the average level of the AOA resonance frequency is shifted down by 2 GHz from 9.8 to 7.8 GHz owing to the slot number increase.

The considered structures with all the $n$ numbers have the second resonance at approximately the same frequency, which is characterized by a lower AOA performance level.

We suppose that the limiting positions of the AOA resonances for very large $n$ can be determined by the resonances of a bilayer of irises having azimuthal "strips of anisotropic conductivity" inclined to the radius.

## 5. Analytical approximation of dihedral bilayer frequency response

In work [17], analytical representations of the reflection and transmission coefficients were obtained for a symmetric two-port network through a set of its eigenfrequencies and due to its S-matrix unitarity. Despite the fact that a pair of conjugated chiral irises does not have longitudinal symmetry, let us check the possibility for these approximate formulas based on the separation of conventionally symmetric and antisymmetric eigen-oscillations to be applied to the conjugated structure. Such structures differ from the longitudinally symmetric geometry by the PP rotation at the output. The actual angle of this rotation can be found numerically from the relevant inhomogeneous boundary value problem solution.

In our case, the reflection and transmission coefficients are approximated as

$$R(f) = -\frac{1}{2}(P^+ + P^-), \quad T(f) = -\frac{1}{2}(P^+ - P^-), \qquad (5)$$

where

$$P^{\pm} = \begin{cases} \prod_{i=1}^{N^{\pm}} \dfrac{\left(\gamma - \overline{\gamma}^{\pm}_{\text{eigen},i}\right)\left(\gamma + \gamma^{\pm}_{\text{eigen},i}\right)}{\left(\gamma - \gamma^{\pm}_{\text{eigen},i}\right)\left(\gamma + \overline{\gamma}^{\pm}_{\text{eigen},i}\right)}, & N^{\pm} > 0, \\ 1, & N^{\pm} = 0, \end{cases}$$

$\gamma = \sqrt{f^2 - f_{\text{cut}}^2}$, $\gamma^{\pm}_{\text{eigen},i} = \sqrt{\left(f^{\pm}_{\text{eigen},i}\right)^2 - f_{\text{cut}}^2}$, $N^{\pm}$ are the numbers of symmetric (for +) and antisymmetric (for −) eigen-oscillations taken into account in the approximation formula, $f^{\pm}_{\text{eigen},i}$ are the corresponding eigenfrequencies, and $f_{\text{cut}}$ is the cutoff frequency of the dominant mode. In our case with a circular waveguide of 16 mm radius, the cutoff frequency is $f_{\text{cut}}(\text{TE}_{11}) = 5.49058$ GHz. The bar above the symbol denotes complex conjugation.

The available analytical representation of the frequency response makes it possible to estimate positions of perfect matching points (PMPs) and, in particular, to predict their merging zone, an important tool in the development of possible polarizers, considering that the merging produces a double-humped broadband response. The condition of PMP merging for the $i$-th and $j$-th neighboring eigenfrequencies is

$$\left(\left|\gamma^{+}_{\text{eigen},i}\right| - \left|\gamma^{-}_{\text{eigen},j}\right|\right)^2 \le \le 4\,\text{Im}\left(\gamma^{+}_{\text{eigen},i}\right)\text{Im}\left(\gamma^{-}_{\text{eigen},j}\right). \qquad (6)$$

Note that the convergence and divergence of the resonance curves (see Fig. 3) generating strong reflection zones or double-humped curves strongly depend not only on the proximity of $\text{Re}\,(f_{\text{eigen}})$ values but on the $Q$-factors of these eigen-oscillations, too.

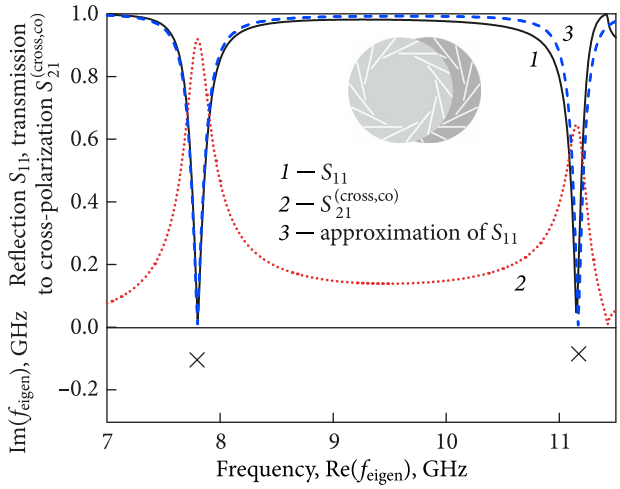


**Fig. 5.** The accurately calculated frequency response (curve 1) and its approximation (curve 3) from formula (5) using the pair of bilayer eigenfrequencies

Fig. 5 compares the results of the scattering problem direct solution by the MMT and the frequency response reconstruction from (5) via two eigenfrequencies. The geometry parameters are $R = 16$ mm, $l = 1$ mm, $t = 0.1$ mm, $n = 14$, $dx = dy = 0$, $a = 12$ mm, and $b = 0.5$ mm. The eigenfrequencies of the rotator with these parameters are

$$f^{-}_{\text{eigen}} = (7.796 - i0.104)\,\text{GHz},$$

$$f^{+}_{\text{eigen}} = (11.171 - i0.085)\,\text{GHz}.$$

The eigenfrequency positions in the complex plane are marked with crosses at negative values of the ordinate axis (Fig. 5). The approximation results are in a very good agreement with the exact calculations in the given case. Note that the eigenvalues

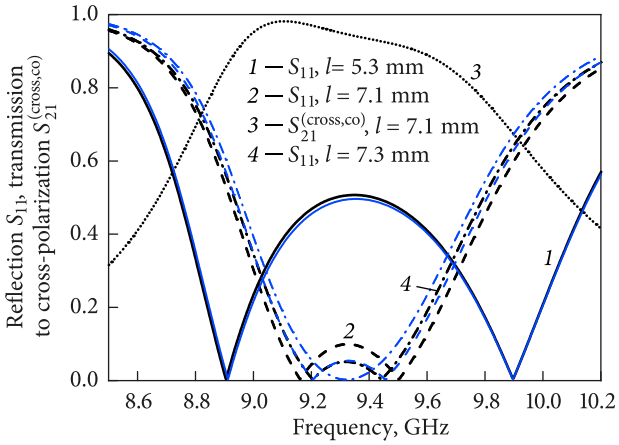


**Fig. 6.** Design of a broadband 14-slot double-layer planar-chiral converter with an internal gap adjustment

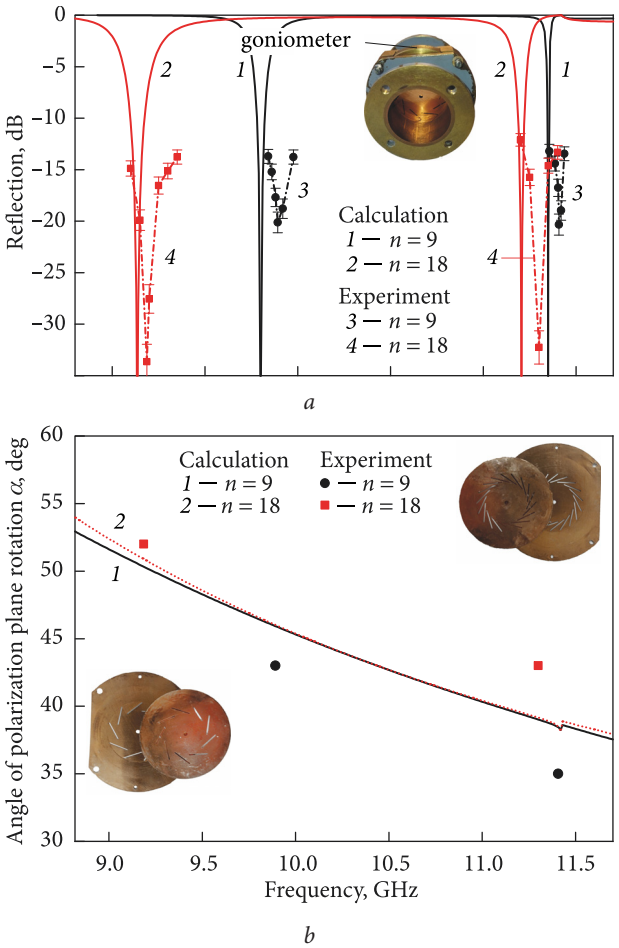


**Fig. 7.** Comparison with experiment for frequency dependences of the reflection coefficient (*a*) and the angle of PP rotation (*b*) for two pairs of irises with 9 and 18 slots

were found by using the same matrix operators as in the scattering problem. The cross-polarized component of the field at the bilayer output is shown with curve *2* (Fig. 5). It has two peaks of the perfect transmission with simultaneous rotation of the PP.

As the two eigenfrequencies become closer, the approximation results differ more and more significantly from the accurate figures. The convergence of the eigenfrequencies can be controlled by varying the bilayer gap. Fig. 6 illustrates the response transformation as the "symmetric" and "antisymmetric" eigen-oscillations get closer. The geometry parameters except $l$ are the same as in Fig. 5. Here, the $\left|\mathrm{Im}\, f_{eigen}^{\pm}\right|$ values are within 0.27 to 0.46 GHz, and both eigen-oscillations have low $Q$-factors. The black color dependences (1, 2, 3, and 4) in Fig. 6 report the accurate results, while the curves of gray shades depict the approximations. Formula (5) approximates the true figures worse if eigen-oscillations have low-$Q$ factors. So, the approximations and the accurate results differ substantially for $l = 7.1$ and 7.3 mm. The approximation curves slightly narrow the band between the PMP pair. As a result, condition (6) is a bit inaccurate for low-$Q$ oscillations ($l = 7.3$ mm). The PMPs obtained by the approximation at $l = 7.3$ mm merge, while the exact curve predicts that the matching bandwidth is of nonvanishing size.

Nevertheless, a good agreement between the approximation and accurate results in the majority of cases shows that based on two eigenfrequencies, some important characteristics of the frequency response can be qualitatively *a priori* predicted. And this is true even if the scatterer does not have longitudinal symmetry.

Fig. 6 further illustrates the possibility of the AOA bandwidth expansion up to 5.3% as two eigenfrequencies converge (see dotted curve *3* for the transmission to the cross-polarized mode).

## 6. Experimental verification

A few pairs of conjugated irises with different numbers of rectangular slots were prepared to experimentally check the theoretical results. The irises were made of copper foil 0.1 mm thick. Rectangular 10 × 0.5 mm slots were burned out by laser. The insets in Fig. 7, *b* give photographic images of two pairs of conjugated irises with 9 and 18 slots. A pair of irises is installed inside a circular waveguide with a 16 mm radius. The rest parameters are $l = 2.77$ mm and $dx = dy = 0$. The distance between the irises is changed by using ring spacers. One iris in the pair can rotate by a desired

angle about the longitudinal axis of the structure. The inset in Fig. 7, *a* gives a photographic image of the waveguide network, the black arrow points at a goniometer with divisions.

The VSWR measurements of the signal reflected from a conjugated pair of irises were conducted versus microwave signal frequency on the experimental setup described in [20]. The confidence interval of the reflection coefficient is determined by the measuring device parameters (Fig. 7, *a*).

The reflection coefficient measurements were carried out using frequency sweeping within 8 to 12 GHz. The frequencies at which the VSWR was a minimum were registered. During transmitted signal measurements, the receiving block with a reflectometer can rotate about the longitudinal axis, enabling us to measure polarization characteristics of the transmitted signal. The measurement results are reported in Fig. 7.

As seen from Fig. 7, *a*, the measurements (dots) and the calculations (solid lines) agree well. For $n = 9$, the minima of the reflection coefficient are observed at frequencies 9.892 and 11.407 GHz in experiment and at 9.800 and 11.349 GHz in theory, with the difference in frequency being 92 and 58 MHz for the low- and high-frequency resonances, respectively. Both resonances therewith are of –20 dB level. For $n = 18$, the reflection coefficient shows a minimum at 9.187 and 11.300 GHz in experiment and at 9.135 and 11.205 GHz in theory. The difference in frequency is 52 and 95 MHz for the low- and high-frequency resonances, respectively. The reflection coefficient amounts –34 dB for the low-frequency resonance and –32 dB for the high-frequency resonance. Hence, the experiment confirms the theoretically made conclusion that the AOA resonance frequencies decrease as the number of rectangular slots increases.

The points in Fig. 7, *b* for the angles of PP rotation correspond to low- and high-frequency resonances of minimum reflection. They agree with the calculations. Some disagreement between the calculation and measurement results may be attributed to inaccuracies in the fabrication and misalignment of the irises.

## Conclusions

1. A sequential chain of eigen-oscillations of planar-chiral objects forming a bilayer with strong optical activity in a circular waveguide has been demonstrated, beginning with slot-aperture oscillations of a single iris and ending with a collective bilayer as a 3D chiral object.

2. A bilayer of conjugated planar-chiral irises with dihedral symmetry of the order $n \geq 3$ has properties of a two-port network. The phases of their reflection and transmission coefficients differ by 90°.

3. If a bilayer only has rotational symmetry, it still creates optical activity bands (e.g., when the first and second layers of the "meta-atom" are not conjugated but identical and angularly twisted). In this case, the bilayer behaves like an asymmetric two-port network with corresponding peculiarities of the frequency response.

4. It has been shown that the frequencies of low-$Q$ symmetric oscillations of a planar-chiral iris belong to the single-mode frequency band of the waveguide, while antisymmetric high-$Q$ eigen-oscillations are very close to the cutoff frequency of the first high-order mode.

5. A strong wave interaction via evanescent fields occurs between the layers when the layer spacing is small. This interaction is the most pronounced when eigenfrequencies of "symmetric" and "antisymmetric" oscillations come close, ending up with the "mode transformation". In the scattering problem context, this manifests itself by forming a relatively broadband zone of good matching.

6. The peculiarity of dihedral bilayers is that the "zone" of strong mutual coupling of the first pair of eigen-oscillations is crossed by the line of 90° PP rotation. It is at these parameters of the object that the AOA manifestation is the most pronounced.

7. The quality factor of optical activity resonances strongly depends on the number of slots in planar-chiral irises. Namely, the $Q$-factor of the first eigen-oscillations and corresponding resonance frequencies decrease as the slot number $n$ increases, particularly at a small iris spacing. This was experimentally verified at the X band and makes it possible to expand the bandwidth of PP rotators under the AOA effect.

8. As in the case of a longitudinally symmetric two-port network, an object with dihedral symmetry of the order $n \geq 3$ admits a simple analytical approximation of the reflection and transmission coefficients by a set of eigenfrequencies.

REFERENCES

1. Rogacheva, A.V., Fedotov, V.A., Schwanecke, A.S., and Zheludev, N.I., 2006. Giant gyrotropy due to electromagnetic-field coupling in a bilayered chiral structure. *Phys. Rev. Lett.*, **97**(17), id. 177401. DOI: 10.1103/PhysRevLett.97.177401
2. Zhao, R., Zhang, L., Zhou, J., Koschny, Th., and Soukoulis, C.M., 2011. Conjugated gammadion chiral metamaterial with uniaxial optical activity and negative refractive index. *Phys. Rev. B*, **83**(3), id. 035105. DOI: 10.1103/PhysRevB.83.035105
3. Song, K., Ding, C., Su, Z., Liu, Y., Luo, C., Zhao, X., Bhattarai, K., and Zhou, J., 2016. Planar composite chiral metamaterial with broadband dispersionless polarization rotation and high transmission. *J. Appl. Phys.*, **120**(24), id. 245102. DOI: 10.1063/1.4972977
4. Zarifi, D., Soleimani, M., and Nayyeri, V., 2012. A Novel Dual-Band Chiral Metamaterial Structure with Giant Optical Activity and Negative Refractive Index. *J. Electromagn. Waves Appl.*, **26**(2—3), pp. 251—263. DOI: 10.1163/156939312800030767
5. Kirilenko, A.A., Steshenko, S.O., Derkach, V.N., Prikolotin, S.A., Kulik, D.Y., Prosvirnin, S.L., and Mospan, L.P., 2017. Rotation of the polarization plane by double-layer planar-chiral structures. Review of the results of theoretical and experimental studies. *Radioelectron. Commun. Syst.*, **60**(5), pp. 193—205. DOI: 10.3103/S0735272717050016
6. Kirilenko, A., Kolmakova, N., Prikolotin, S., and Perov, A., 2013. Simple example of polarization plane rotation by the fringing fields interaction. In: *Proc. EuMW*, 6—10 Oct. 2013, Nuremberg, Germany. IEEE, 2013, pp. 936—938.
7. Kirilenko, A.A., Steshenko, S.O., Derkach, V.N., Ostrizhnyi, Y.M., and Mospan, L.P., 2020. Tunable polarization rotator on a pair of grooved flanges. *J. Electromagn. Waves Appl.*, **34**(17), pp. 2304—2316. DOI: 10.1080/09205071.2020.1812442
8. Giloan, M., Gutt, R., and Saplacan, G., 2015. Optical chiral metamaterial based on meta-atoms with three-fold rotational symmetry arranged in hexagonal lattice. *J. Opt.*, **17**(8), id. 085102. DOI: 10.1088/2040-8978/17/8/085102
9. Bai, B., Svirko, Y., Turunen, J., and Vallius, T., 2007. Optical activity in planar chiral metamaterials: Theoretical study. *Phys. Rev. A*, **76**(2), id. 023811. DOI: 10.1103/PhysRevA.76.023811
10. Kirilenko, A.A., Steshenko, S.O., Derkach, V.N., and Ostryzhnyi, Y.M., 2019. A tunable compact polarizer in a circular waveguide. *IEEE Trans. Microw. Theory Tech.*, **67**(2), pp. 592—596. DOI: 10.1109/TMTT.2018.2881089
11. MacPhie, R.H., and Wu, K.L., 1995. Scattering at the junction of a rectangular waveguide and a larger circular waveguide. *IEEE Trans. Microw. Theory Tech.*, **43**(9), pp. 2041—2045. DOI: 10.1109/22.414538
12. Kirilenko, A.A., Steshenko, S., and Ostryzhnyi, Y., 2020. Topology of a Planar-chiral Iris as a Factor in Controlling the "Optical Activity" of a Bilayer Object. In: *2020 IEEE Ukrainian Microwave Week (IEEE UkrMW):* proc., 21—25 Sept. 2020, Kharkiv, Ukraine, 2020, pp. 555—558.
13. Kolmakova, N.G., Perov, A.O., Senkevich, S.L., and Kirilenko, A.A., 2011. Abnormal propagation of EMW through below cutoff holes and intrinsic oscillations of waveguide objects and periodic structures. *Radioelectron. Commun. Syst.*, **54**(3), pp. 115—123. DOI: 10.3103/S0735272711030010
14. Kirilenko, A.A., and Perov, A.O., 2008. On the common nature of the enhanced and resonance transmission through the periodical set of holes. *IEEE Trans. Antennas Propag.*, **56**(10), pp. 3210—3216. DOI: 10.1109/TAP.2008.929437
15. Kirilenko, A.A., Steshenko, S.O., Derkach, V.N., and Ostrizhnyi, Y.M., 2019. Comparative analysis of tunable compact rotators. *J. Electromagn. Waves Appl.*, **33**(3), pp. 304—319. DOI: 10.1080/09205071.2018.1550443
16. Mackay, A., 1989. Proof of polarization independence and nonexistence of crosspolar terms for targets presenting with special reference to rotational symmetry frequency-selective surfaces. *Electron. Lett.*, **25**(24), pp. 1624—1625. DOI: 10.1049/el:19891088
17. Kirilenko, A.A., and Tysik, B.G., 1993. Connection of S-matrix of Waveguide and Periodical Structures with Complex Frequency Spectrum. *Electromagnetics*, **13**(3), pp. 301—318. DOI: 10.1080/02726349308908352
18. Melezhik, P.N., Poyedinchuk, A.Y., Tuchkin, Y.A., and Shestopalov, V.P., 1988. About analytical origins of eigenmode coupling. *Sov. Phys. Dokl.*, **300**(6), pp. 1356—1359.
19. Yakovlev, A.B., and Hanson, G.W., 1998. Analysis of mode coupling on guided-wave structures using Morse critical points. *IEEE Trans. Microw. Theory Tech.*, **46**(7), pp. 966—974. DOI: 10.1109/22.701450
20. Kolmakova, N., Prikolotin, S., Perov, A., Derkach, V., Kirilenko, A., 2016. Polarization plane rotation by arbitrary angle using D4 symmetrical structures. *IEEE Trans. Microw. Theory Tech.*, **64**(2), pp. 429—436. DOI: 10.1109/TMTT.2015.2509966

*Received 04.12.2023*

*А.О. Кириленко[1,2], С.О. Стешенко[1,2], Є.М. Остріжний[1], В.М. Деркач[1]*

[1] Інститут радіофізики та електроніки ім. О.Я. Усикова НАН України
вул. Акад. Проскури, 12, м. Харків, 61085, Україна
[2] Харківський національний університет імені В.Н. Каразіна
майдан Свободи, 4, м. Харків, 61022, Україна

ВЛАСНІ КОЛИВАННЯ В ПЛАНАРНО-КІРАЛЬНИХ ДВОШАРОВИХ ОБ'ЄКТАХ ПОРОДЖУЮТЬ ШТУЧНУ ОПТИЧНУ АКТИВНІСТЬ

**Предмет і мета роботи** — дослідження впливу топології окремих компонентів планарно-кірального двошарового об'єкта, що складається з пари спряжених діафрагм з прямокутними щілинами у круглому хвилеводі, на його резонансні частоти, добротність резонансів та на здатність обертати площину поляризації.

**Методи та методологія.** Усі чисельні результати були отримані за допомогою власного програмного забезпечення MWD-03 на основі методу часткових областей і методу поперечного резонансу.

**Результати.** На прикладі хвилеводу показано, що внутрішня структура окремих компонентів і діедральна симетрія спряженого бішару дозволяють поширити висновки спектральної теорії (теорії власних коливань) на всі такі об'єкти. З іншого боку, вони поводяться як симетричні двопортові хвилевідні вузли з умовними «симетричними» та «антисиметричними» власними коливаннями. Взаємний вплив цих власних коливань залежить від параметрів бішару, і саме в зоні зближення їх частот досягаються максимальний поворот площини поляризації і найширша смуга пропускання. Показано, що збільшення кількості щілин зменшує резонансну частоту. Теоретичні результати підтверджені експериментальними вимірюваннями, проведеними для пар спряжених діафрагм з різною кількістю прямокутних щілин в *X*-діапазоні частот.

**Висновки.** Пара спряжених кіральних діафрагм може використовуватися для обертання площини поляризації. Топологія діафрагм, відстань між ними і взаємний кут повороту впливають на резонансні частоти. Знизити резонансні частоти можна, збільшуючи довжину прямокутних щілин і/або їх кількість. Незважаючи на відсутність поздовжньої симетрії, такі об'єкти мають властивості двопортових хвилевідних вузлів. Зокрема, фазовий зсув їх коефіцієнтів відбиття і проходження за модулем становить 90°. До того ж можливість поділу власних коливань на умовні «симетричні» і «антисиметричні» за близькістю їх полів до полів коливань відповідної симетрії дозволяє використовувати наближені формули для апроксимації коефіцієнтів відбиття і проходження через власні частоти.

***Ключові слова:*** *власні коливання, двошарові об'єкти, 3D-кіральність, штучна оптична активність, діедральна симетрія, планарно-кіральні діафрагми, перетворювачі поляризації.*